Journal of Molecular Structure 1245 (2021) 131058

Contents lists available at ScienceDirect

Journal of Molecular Structure

journal homepage: www.elsevier.com/locate/molstr

Carboxylato bridging Cu(II) coordination polymer: Structure, magnetism and catalytic reduction of nitrophenols

Srikanta Jana[a], Suhana Karim[b], Sukanya Paul[a], Ennio Zangrando[c], M. Salah El Fallah[d,*], Debasis Das[b,*], Chittaranjan Sinha[a,*]

[a] Department of Chemistry, Jadavpur University, Jadavpur, Kolkata 700032, India
[b] Department of Chemistry, University of Calcutta, Kolkata 700009, West Bengal, India
[c] Department of Chemical and Pharmaceutical Sciences, University of Trieste, Via L. Giorgieri 1, 34127 Trieste, Italy
[d] Departament de Química Inorgànica i Organica, Secció de Química Inorgànica, Universitat de Barcelona, Martí i Franquès, 1-11, 08028-Barcelona, Spain

ARTICLE INFO

Article history:
Received 2 June 2021
Revised 29 June 2021
Accepted 5 July 2021
Available online 9 July 2021

Keywords:
Coordination polymer
Magnetic study
Hand-grinding
Nano – material
Nitro phenol reduction

ABSTRACT

The 1D coordination polymer, $[Cu_2(\mu_2\text{–}OH)_2(DABA)_2]_n$ (**1**), (HDABA = 4-Diallylamino-benzoic acid) is characterized by Single crystal X-Ray diffraction analysis. The structure switches to a 2D geometry by hydrogen bonding interactions. Hand grinding aqueous suspension of the coordination polymer, **1**, present in nano regime of *av*. 100 nm dimension and shows catalytic performance in the reduction of toxic nitrophenols to corresponding aminophenols by $NaBH_4$. The rate constant values (κ_{app}) are 2.4×10^{-3} (4-NP), 5.3×10^{-3} (2,4-DNP) and 5.6×10^{-3} (2,4,6-TNP) s^{-1} are much higher than reduction by only $NaBH_4$. The susceptibility measurements ($\chi_M T$) of Cu(II) coordination polymer indicates the presence of a very weak antiferromagnetic coupling between the metal centres. The hand grinding technique and reusability of **1** makes the approach chemically green, cost effective and attracts the attention towards the real-life application.

1. Introduction

Nitroaromatics (NACs) are well known weedkillers and insect repellent and precursors to synthetic dyestuff [1–3]. These compounds are not degraded easily by microbes. Because of strong toxicity, the NACs are noted as pollutants by the Environmental Protection Agency [4]. Conventional waste water management methods such as reverse osmosis, adsorption ion exchange [5], photocatalysis [6], membrane separation [7], and electro-coagulation have been proposed for the detoxification of highly persistent organic pollutants. Besides, some of the nitrophenols are explosive and have been used for terroristic activity. Immediate disposal of NACs is an issue of explosive and safety departments of the Government. The conversion of toxic NACs to the secondary nontoxic and useful chemicals is very urgent issue for the forensic personals and researchers. The chemical reduction has been one of the most commonly applied techniques of detoxification of the NACs using metal nanoparticles (MNP's) as catalysts and BH_4^- as reducing agent. On the other hand, the reduced products, amino phenols (AP) are very important moiety in dyes and pigments, pharmaceuticals industry [8]. Literature survey reports that there is no such coordination polymer that serves as catalyst bed for the reduction of NACs. Up to now, large number of nano metal catalysts (Pt, Au, Ag, Pd etc.) have been fabricated for the reduction of NACs [9–13]. Yongsheng Fu [14] et al. (2017), Nguyen [15] et al. (2018) and Yukui Fu [16] et al. (2019) have used expensive gold catalyst to carry out such transformation while Ying Ma [17] et al. (2017) used silver catalyst for the same. Sahiner [18] et al. (2010) introduced cobalt catalyst for the reduction.

Coordination Polymers (CPs) are prepared by bridging organic coordinating groups with metal ions [19–22]. They are promising contender for catalysis [23], drug delivery [24], gas storage [25], and energy storage systems [26,27]. Some of the CPs have been serving as catalyst in the reduction of Nitrophenols (NP), (4-NP, 2,4-DNP, 2,4,6-TNP) [28]. In this paper, we have characterized Cu(II) coordination polymer (CP) that has been used as a catalyst for the reduction of toxic and explosive NPs in aqueous medium. The easy removal of solid phase catalyst even at nM level by filtration makes this catalyst analytically useful. The efficiency of the catalyst is reflected in the rate constant (κ_{app}) data of the nitrophenol reductions, which is larger than the conventional methods (**Table S1**). Owing to the catalytic activity we have designed the coordi-

* Corresponding author.
E-mail addresses: salah.elfallah@qi.ub.edu (M.S.E. Fallah), dasdebasis2001@yahoo.com (D. Das), crsjuchem@gmail.com (C. Sinha).

https://doi.org/10.1016/j.molstruc.2021.131058

nation polymer of Cu(II)- 4-diallylamino benzoic acid and has been structurally characterized. The reusability of the catalyst in the several catalytic cycles of various nitrophenols, makes the compound unique. Besides, the coordination polymer of Cu(II), d^9, may show efficient magnetic exchange behaviour that has been supported by variable temperature magnetic measurements. A comparison of recently reported results in Carboxylato bridging Cu(II) complexes has been documented in **Table S2**.

2.1. Experimental methods and materials

The chemicals required in this research were obtained from Sigma Aldrich and no further purification was carried out. Microanalytical data (C, H, N) were collected using Perkin-Elmer 2400 CHNS/O elemental analyser. Perkin–Elmer Pyris Diamond TG/DTA instrument was used for thermogravimetric analysis in the temperature range 30 - 600 °C under N_2 atmosphere at a heating rate of 12 °C min^{-1}. Bruker D8 advance X-ray diffractometer was used for field emission scanning electron microscope (FESEM, S-4800, Hitachi) measurement. The PXRD data were collected on an X-ray diffractometer using Cu Kα radiation (λ = 1.548 Å) generated at 40 kV and 40 mA. The PXRD spectra were recorded in a 2θ range of 5–50°. Magnetic susceptibility measurement for the compound was carried out on polycrystalline sample, at the Servei de Magnetoquímica of the University de Barcelona, with a Quantum Design SQUID MPMS-XL susceptometer apparatus working in the range 2–30 K and 30–300 under magnetic field of approximately 500 G and 10,000 G, respectively. Diamagnetic corrections were estimated from Pascal Tables.

2.2. Synthesis of coordination polymer (CP, 1)

4-Diallylamino benzoic acid (HDABA) was prepared by reported procedure [29]. An ethanolic solution of (2 ml) of HDABA (43.45 mg, 0.2 mmol) neutralized with Et_3N (20.23 mg, 0.2 mmol) was added slowly in drops to water–methanol (1:1, v/v) buffer mixed solvent over the aqueous solution (2 ml) of $Cu(NO_3)_2.3H_2O$, (48.32 mg, 0.2 mmol) [30]. After week long settling needle-shaped blue coloured crystals were grown on the glass wall. The crystals were isolated mechanically under the microscope and washed several times with methanol and water (1:1) mixture, and dried in a desiccator. The yield of product, $[Cu_2(\mu_2\text{–}OH)_2(DABA)_2]_n$ (**1**) was 85% (78.23 mg).

Elemental analysis, Calculated ($C_{26}H_{30}Cu_2N_2O_6$): C, 52.61; H, 5.09; N, 4.72%; Found: C, 52.52; H, 5.0; N, 4.76%. FT-IR (4000−400 cm^{-1}) (**Fig. S1**): 3388 (w), 1637 (s), 1594 (s), 1537 (s), 1385 (s), 1351 (s), 1251 (s), 1199 (s), 1136 (s), 994 (s), 912 (s), 817 (s), 784 (s), 703 (s), 641 (s), 555(w), 512 (w).

2.3. X-Ray crystallographic data collection and structure determination

Bruker Smart Apex diffractometer equipped with CCD and Mo-Kα radiation (λ = 0.71073 Å) was used for crystal data collection of **1** (**Table S3**) at room temperature. Cell refinement, indexing and

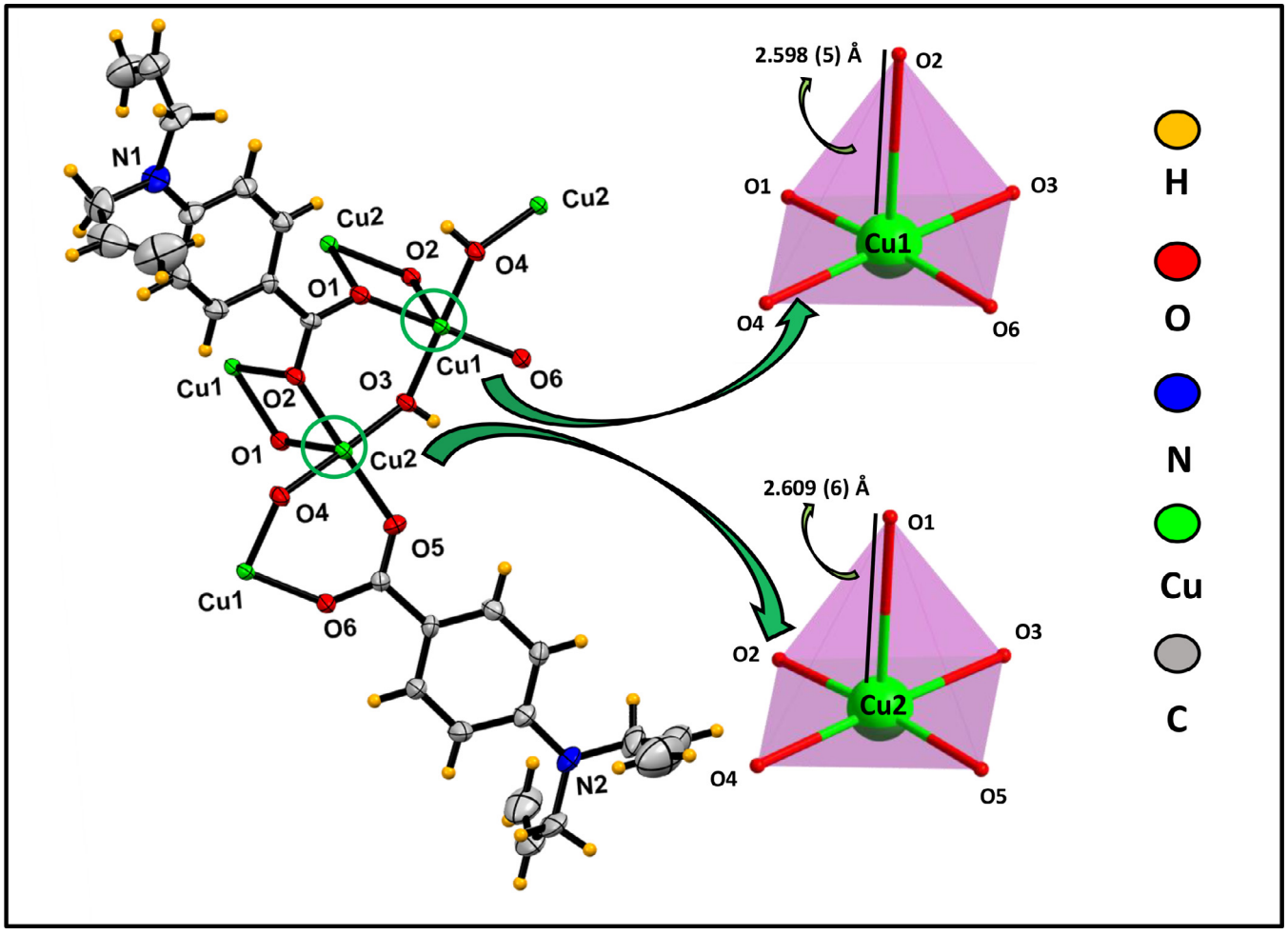

Fig. 1. ORTEP diagram of coordination polymer $[Cu_2(\mu_2\text{–}OH)_2(DABA)_2]_n$ (1) (40% probability ellipsoids).

scaling of the data were done by using programs of Bruker Smart Apex and Bruker Saint packages [31]. Direct method used for the structure analysis with subsequent Fourier analyses [32] and refined by the full-matrix least-squares method based on F_0^2 with all observed reflections [33]. Hydrogen atoms were placed at geometrical positions. All the calculations were performed using the WinGX System, Ver 2018.3.39 Molecular pictures were prepared with program DIAMOND [34].

2.4. Preparation of nanoscale cu(ii) coordination polymer (1)

Solubility of the coordination polymer in common organic solvent and in aqueous medium is a practical problem. There are so many other methods like sonochemical, surfactant mediated synthesis, solvothermal, microemulsion etc. to scale down the particle size but all of them consume time and are non-ecofriendly. So, to handle this problem we take the help of a green hand-grinding strategy [35, 36]. By applying this classical technique the particle size of the CP, **1**, came down to 100 nm and surface area would increase accordingly. The compound **1** (50 mg) was grinded with the help of mortar pestle for near about 45 mins and extracted with water. The relevant experiments were performed using the aqueous extract. To confirm the structural integrity and morphology in nano regime the prepared material was analysed by measuring PXRD. The phase purity of the nano scaled product (**1**) matches with the PXRD patterns as that of the synthesized ones.

2.5. Reduction of nitrophenols using $NaBH_4$ catalysed by nano regime 1

The reduction of nitrophenols (4-NP, 2,4-DNP, 2,4,6-TNP) to corresponding aminophenols were followed by Shimadzu UV- 3101 PC UV-Visible spectrophotometer. In a cuvette, nitrophenol (30 μl of 10 mM) in deionized water (3 ml) was added to $NaBH_4$ (0.16 ml of 0.1 M) solutions followed by the addition of water dispersed nano scaled synthesized compound **1** (1 mg). The solution colour slowly changed from bright yellow to transparent as the reaction proceeds with time. The colour change was followed by spectral measurement with time. Pseudo-first order rate equations were used to calculate the kinetic data.

3. Results and discussion

3.1. Molecular structure

The compound **1** crystallizes in the orthorhombic space group, *F*dd2 and the symmetric unit comprises two independent Cu(II), two 4-(diallylamino)benzoate ($DABA^-$) bridgers and two μ_2–OH^-. Two copper atoms, Cu1 and Cu2, exhibit distorted square pyramidal geometry where the basal plane is formed by two bridging hydroxides and two carboxylato oxygen donors (Fig. 1 and **Fig. S2**). The coordination is completed by occupying caoboxylato-O at apical position of a symmetry related species. The coordination bond lengths and angles, reported in **Table S4**, indicate that the Cu-O bond distances in the square pyramidal base are in between 1.875(6)−1.988(4) Å, while the Cu-O (apical) are significantly longer of 2.598(5) A and 2.609(6) A, for Cu1 and Cu2, respectively.

The 1D polymer (Fig. 2**a**) is formed by two adjacent -$[Cu(DABA)(OH)]_n$- chains where carboxylate-O, O1 and O2, behave as apical donors for the copper atoms to the adjacent chain. In chain, copper atoms are alternatively separated by 3.338 and 3.377 Å, sharing a vertex of the square pyramidal polyhedron (Fig. 2**b**). Besides, copper atoms of the two adjacent chains are 3.389 Å far apart and share an edge of their polyhedra.

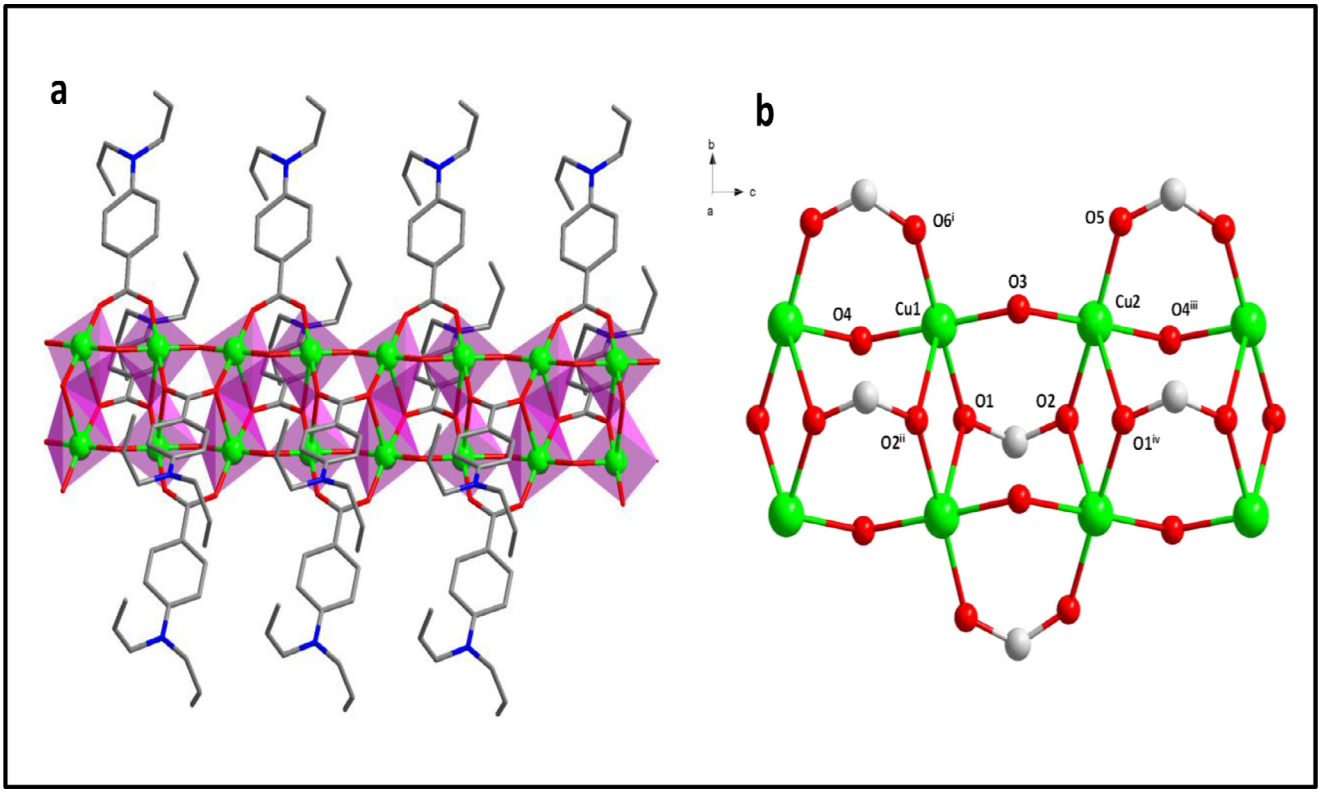

Fig. 2. (a) The two connected 1D polymeric chains elongated along axis c with indication of coordination polyhedral around the copper atoms (H atoms not included for clarity) and (b) Details of the 1D chain of 1.

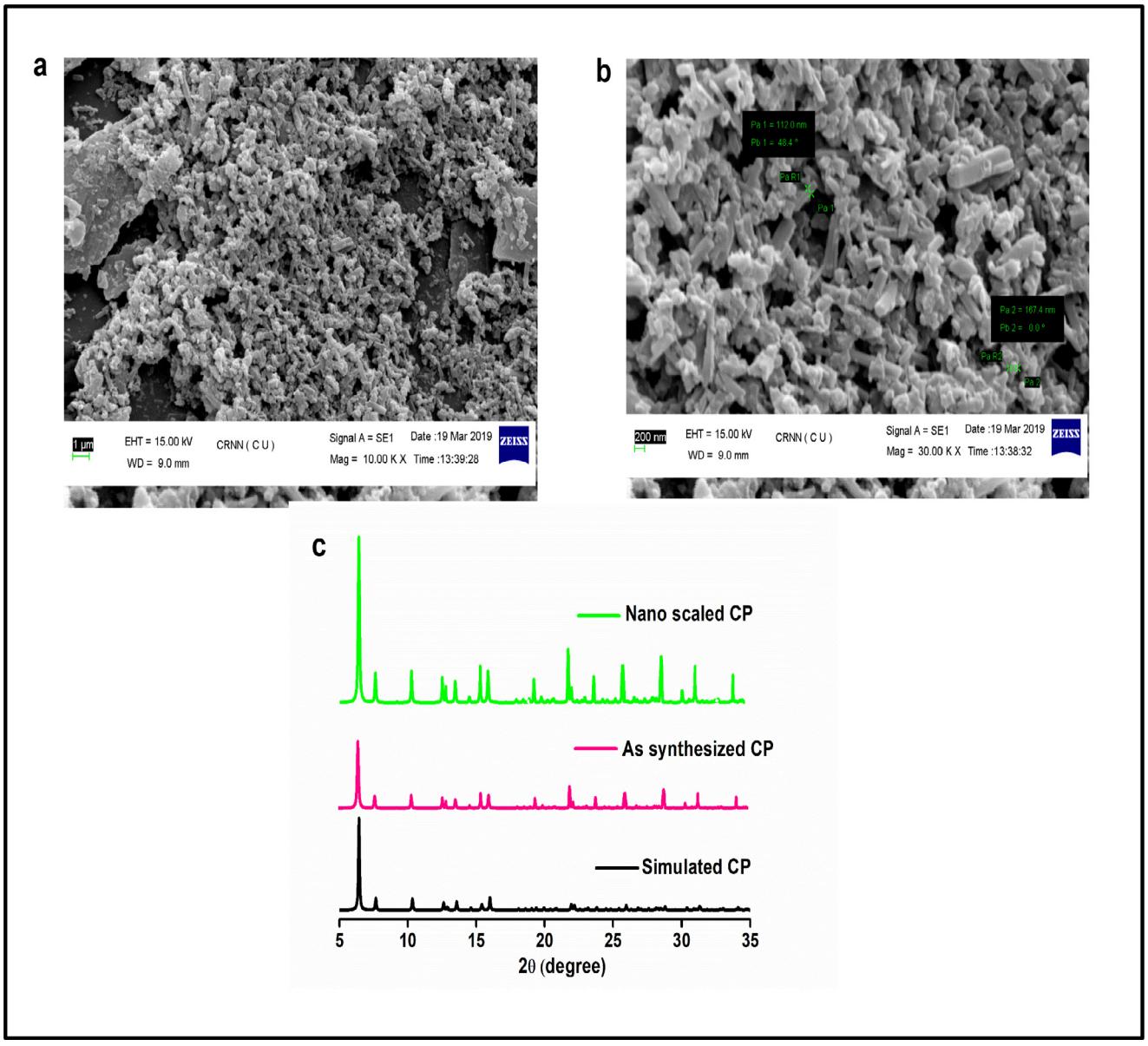

Fig. 3. (a) Low magnificent SEM image of synthesized nano scaled compound 1. (b) High magnificent cubic rod-shaped SEM image of nano scaled compound 1. (c) PXRD pattern of simulated, as synthesized & nano scaled product 1 collected under air.

3.2. Stability and morphology of 1

The particle size of the synthesized compound, **1**, diminished to nano regime by following hand grinding technique. The resultant powder **1** was characterised by scanning electron microscope. The SEM images of the powder **1** had a cubic rod like morphology (**Fg. 3a**) as it is supported from the single crystal symmetry of **1**. The SEM image (Fig. 3**b**) reveals the uniform distribution of the particles. Using Gaussian function, we have fitted the particle size distribution which is obtained from the SEM images. The fittings show that the average particle size is 100 nm (**Fig. S3**). Small particle size indicates the lower grain size and higher grain boundary which may affect the conducting electrons which helps in the reduction reaction. Intense peaks of PXRD patterns of bulk are matched with those simulated from single crystal data and nano regime form which also indicates the phase pureness of the bulk sample (Fig. 3**c**).

Thermogravimetric analysis (TGA) of nano scaled compound has shown that, the compound is stable up to 420 K after decomposition (**Fig. S4**), the end product of the thermal decay (near about 26%) may be the copper oxide and this is in support of the calculated data (CuO, 26.78%).

3.3. Magnetic studies

Bridged Cu(II) (d^9) multinuclear complexes usually show weak magnetic exchange between spins and is the reason for subnormal magnetic moment and/or antiferromagnetic coupling. In this work, the magnetic measurements were carried out at 2 – 300 K to analyse the effect of temperature on the spin population at higher magnetic levels.

The plot of $\chi_M T$ against T [χ_M is the magnetic susceptibility per two copper(II) ions] (Fig. 4) shows that at 300 K, $\chi_M T$ is 0.90 $cm^3\ mol^{-1}$ K, a value which was as expected for magnetically isolated spin doublets (0.75 cm^3 K mol^{-1} with $g = 2.0$). This value was kept upon cooling until 40 K and it further decreased to 0.177 $cm^3\ mol^{-1}$ K at 2 K. This small decrease in the low temperature region could be characteristic to a very weak intramolecular antifer-

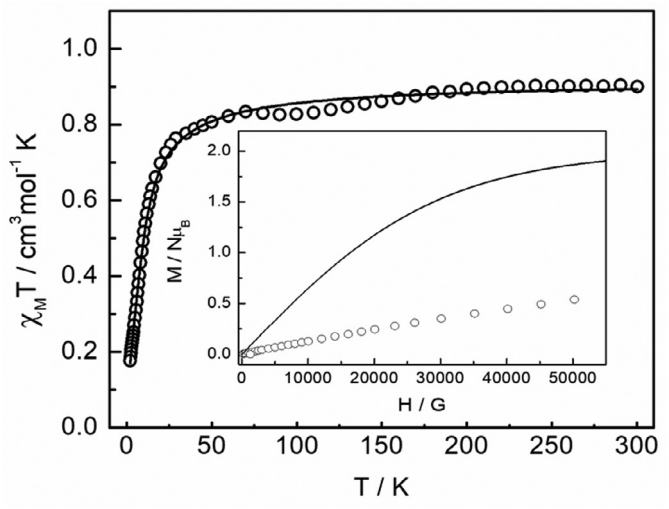

Fig. 4. Variation of $\chi_M T$ vs T for compound 1 (per two Cu). Figure in Inset refers to the field dependence of reduced magnetization at 2 K for 1 (per two Cu), continuous line corresponds to the Brillouin function simulation for two isolated ions with $S = 1/2$ and $g = 2.0$.

romagnetic coupling across the chelated ligand (copper•••copper separation alternately of 3.338 and 3.377 Å) [37].

The structure consists of copper ions bridged by 4-(diallylamino)benzoate ($DABA^-$) through the oxygen atoms (Fig. 5), giving a system with a ladder like chain motif. The interpreta-

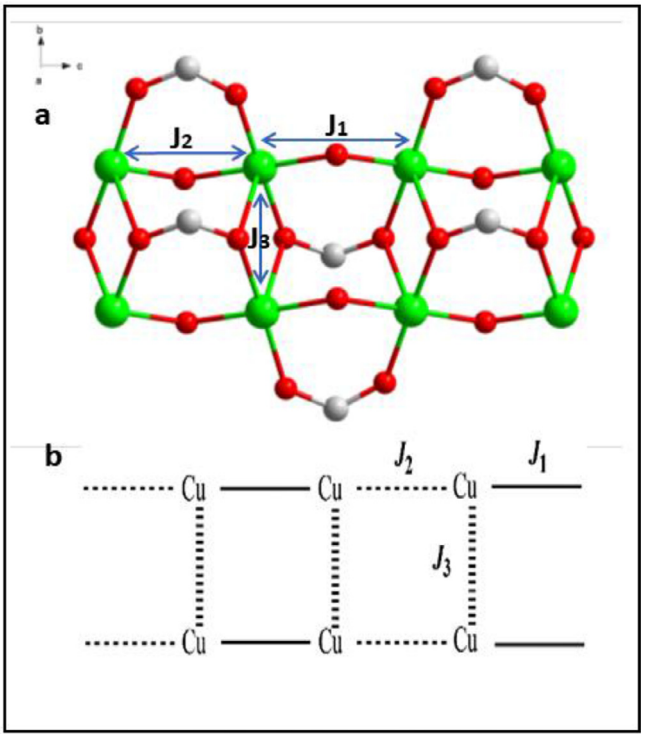

Fig. 5. Schematic diagram representing the exchange interaction within Cu(II) centres of 1; (a) structure motif and (b) metal skeleton for magnetic exchange.

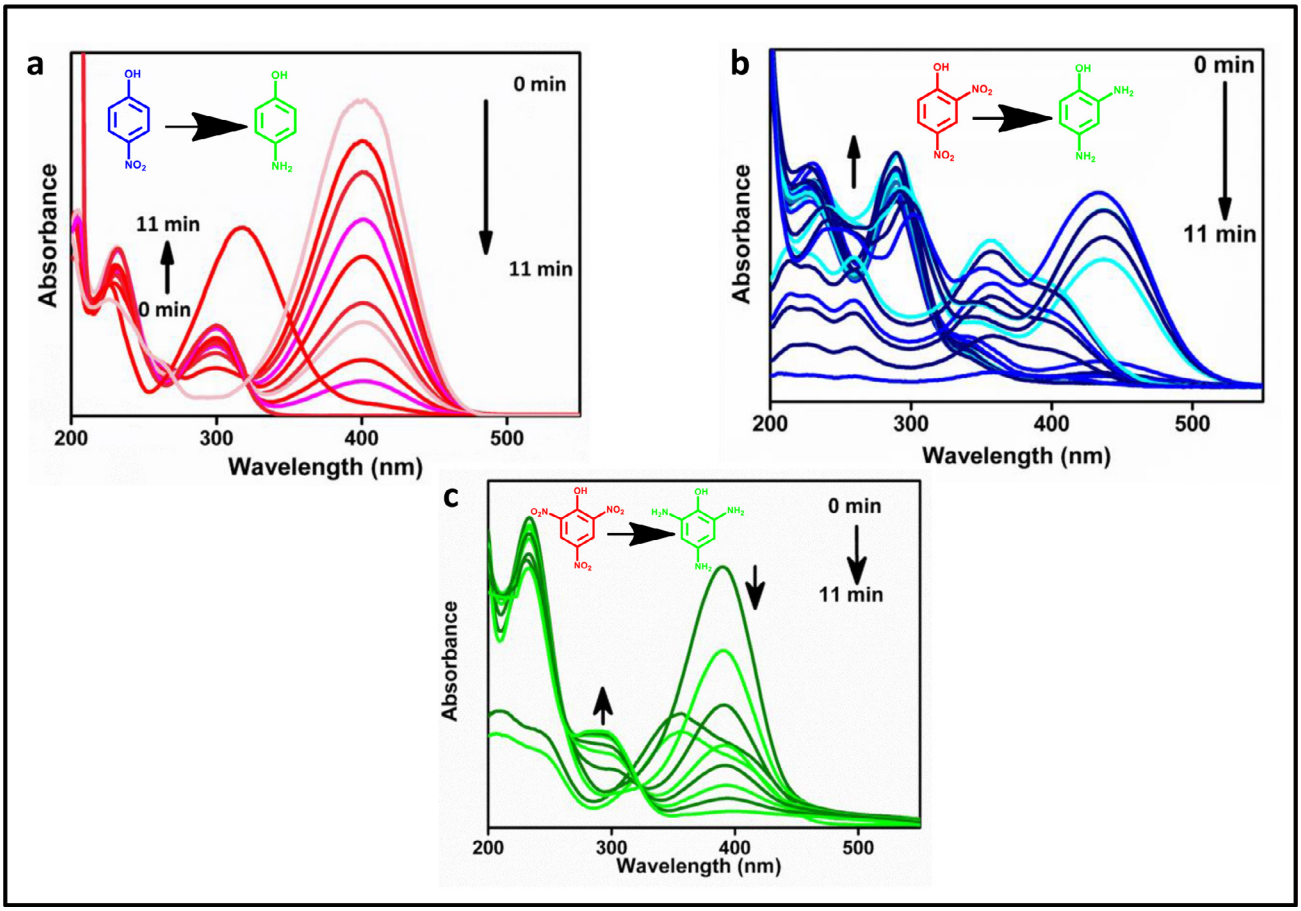

Fig. 6. Time-dependant UV–vis spectral changes in Nitro Aromatic Compounds like (a) 4-nitrophenol (4-NP), (b) 2,4-dinitrophenol (2,4-DNP), (c) 2,4,6-trinitrophenol (2,4,6-TNP) in presence of 1 and excess $NaBH_4$.

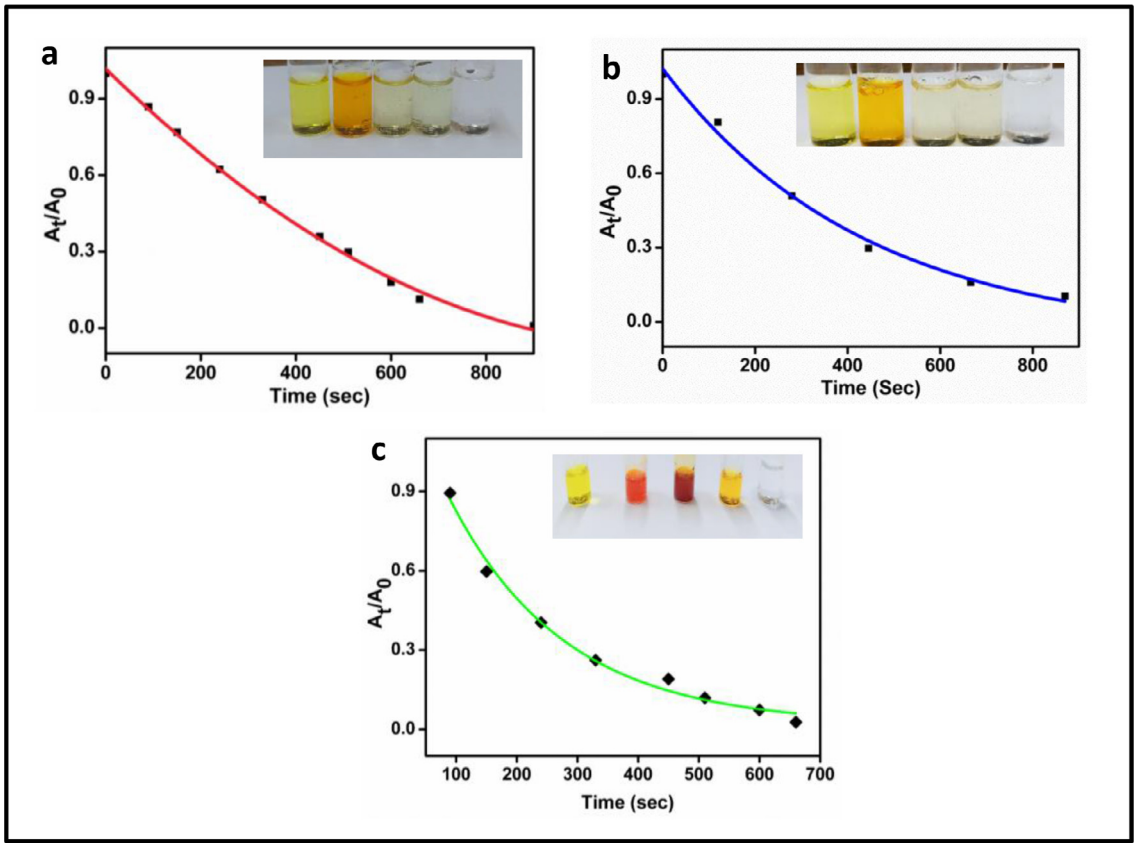

Fig. 7. Concentration (A_t/A_0) changes in (pink solid line, nude eye test inserted in the box) 4-nitrophenol, (blue solid line) 2,4-dinitrophenol and green solid line) 2,4,6-trinitrophenol in the presence of catalyst 1.

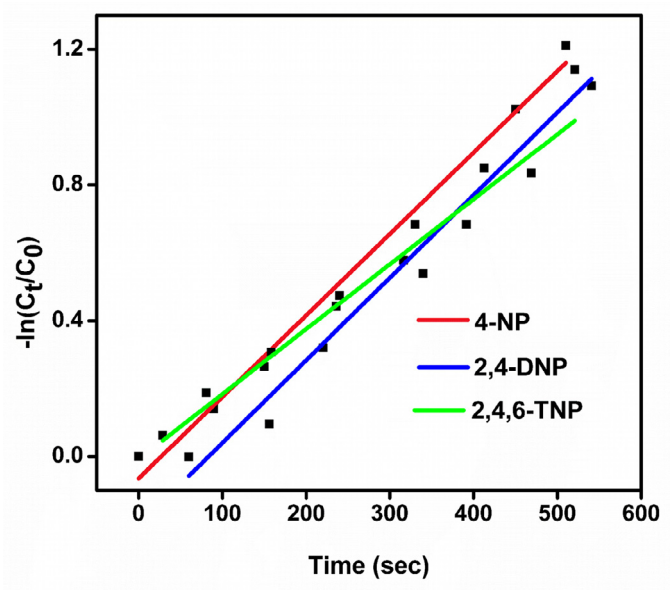

Fig. 8. The plot of ln (C_t/C_0 vs t (time) for 4-nitrophenol (pink solid line), 2,4-dinitrophenol (blue solid line) and 2,4,6-trinitrophenol (green). C_t, the concentration of NPs at time t and C_0, the initial concentration of nitrophenols at $t = 0$. The C_t/C_0 is measured from the relative intensity of absorbence (A_t/A_0).

tion of magnetic behaviour of **1** is attended by considering two assumption: (*i*) a negligible contribution from the weak axial interactions through one of the 4-(diallylamino)benzoate due to the large Cu(1)-O(2) and Cu(2)-O(1) distances (2.597 Å and 2.608 Å respectively) then $J_3 = 0$ (Fig. 5**a**, 5**b**), (*ii*) the very similar Cu1 and Cu2 geometric environment (mainly the neighbours angles Cu-O-Cu which are 123.67° and 126.71° (*vide* detailed crystallographic data).

Use of one coupling parameter ($J = J_1 = J_2$) must be considered to assess the possible magnetic interaction corresponding to the double oxo/carboxylato bridge. The magnetic data have been fitted using Bonner-Fisher calculation [37] based on the isotropic Heisenberg Hamiltonian: $H = -J\ \Sigma(S_iS_{i+1})$. The best fit parameters from 300 down to 2 K are found as $J = -8.07\ cm^{-1}$ and $g = 2.07$ with an error $R = 2.7 \times 10^{-4}$, where $R = \Sigma[(\chi_M T)_{exp} - (\chi_M T)_{calc}]^2/\Sigma[(\chi_M T)_{exp}]^2$ (Fig. 4). The small value of the super-exchange parameter can be realised on considering the large Cu-O-Cu angle (123.7°/126.7°). The weak antiferromagnetic interaction was checked by magnetization measurements at 2 K up to an external field of 5 T. The magnetization in M/N_β units at higher field indicates a value of 0.54 corresponding to two isolated Cu (II) ions (Fig. 4**, inset**). The shape of the plot is compared with the Brillouin plot (solid line plot) for two isolated ions with $S = 1/2$ system and $g = 2$; this indicates the slower magnetization which is consistent with a weak antiferromagnetic interaction.

3.4. Reduction of nitrophenols

The nano regime form of the coordination polymer, **1**, acts as a competent catalyst in the reduction of toxic nitrophenols to non-toxic *p*-aminophenols compared to free Cu(II) salt while the crystalline compound **1** is insoluble in water. The Coordination polymer nano materials (CPNM) is a new advanced area in nanoscience and nanotechnology in the last decade and have shown many applications in the field of catalysis, medicine, bioimaging, drug delivery, sensors in biomedicine, e-skin, energy harvester, etc. [38–40]. During the reduction of 4-NPs, $NaBH_4$ serves as a reducing

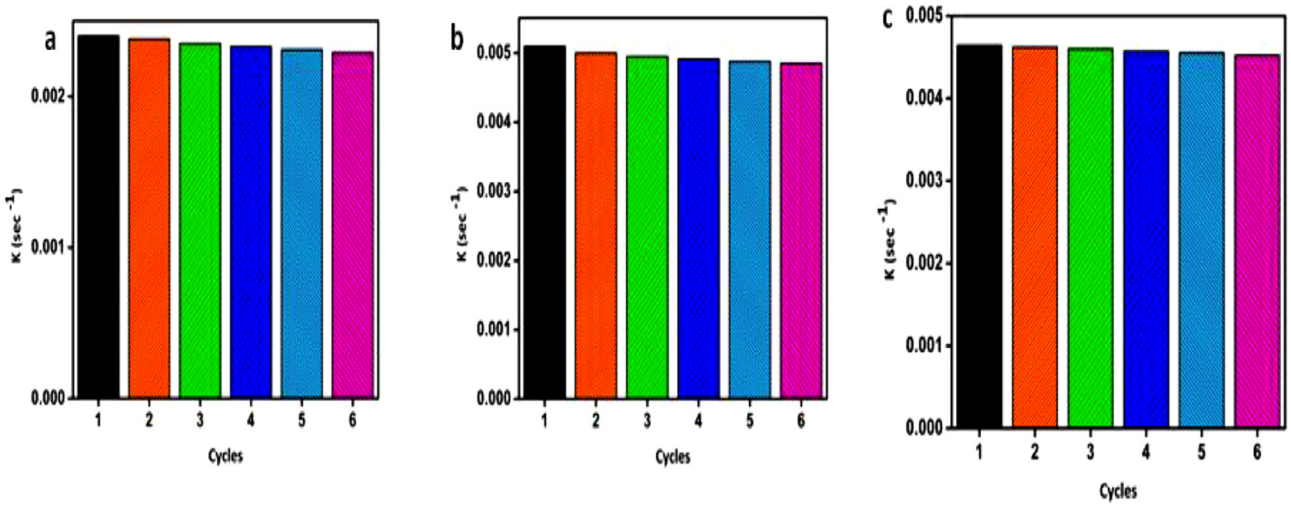

Fig. 9. Reusability cycles of (a) 4-NP, (b) 2,4-DNP and (c) 2,4,6-TNP.

agent and nano regime coordination polymer, **1** serves as a catalyst. In absence of catalyst, the reaction is unfavourable and no significant spectral change is seen even after 4 h (**Fig. S5**); the nano scaled compound plays a significant role to bring reactant and reagent together during the catalysis and improves the transfer of electrons from BH_4^- to the nitro groups of 4-NPs [41–46]. The nano catalyst surface may decrease the kinetic energy barrier and hence makes easy to reduction.

Upon addition of $NaBH_4$ to NP solution, colour turned from yellow to bright yellow. The strong absorption peak at 317 nm is shifted to 401 nm (Fig. 6**a**); this may be due to the generation of nitrophenolate anions under basic condition and the absorbence remained intact with time in the absence of a nano scaled catalyst **1** but decreased rapidly with a small amount of the catalyst.

The absorption peak at 357 nm in case of 2, 4-dinitrophenol (2, 4-DNP, Fig. 6**b**) decreases with concomitant increase in absorption at 450 nm (by adding $NaBH_4$ in reaction medium) with time followed by the decrement of intensity at 450 nm band with subsequent development of new band at 300 nm. This implies that the two step reduction reaction: 2, 4-dinitrophenol → intermediate 2-amino-4-nitrophenol → 4-aminophenol. 2,4,6-Trinitrophenol (2,4,6-TNP) undergoes reduction similarly. Herein, the peak (Fig. 6**c**) at 389 nm corresponds to phenolate anion and the peak at 291 nm increases with time indicates the formation of 2,4,6-triaminophenol.

The pseudo first-order kinetics principle is used and it is more appropriate to assess the rate constants data for nitrophenol reduction because the concentration of $NaBH_4$ is higher than those of model substrate and can be considered as a constant during the reaction period (Fig. 7). The linear relationship of ln (A_t/A_0) versus time (t) indicates that the reduction of nitrophenols by nano scaled catalyst **1** follows the pseudo first order kinetics. The rate constants for 4-nitrophenol, 2,4-dinitrophenol and 2,4,6-trinitrophenol reduction are 0.0024 s^{-1}, 0.0053 s^{-1}, and 0.0056 s^{-1} respectively (Fig. 8).

3.5. Reusability test

The catalyst was separated after reaction by filtration method then reuse the catalyst at least 6 times (Fig. 9). After catalytic performance, we did the SEM experiment to check its integrity (**Fig. S6-S8**) which exactly matches with the SEM image before the catalytic activity. We also performed PXRD experiment after separating the catalyst. The peak-to-peak matching elaborates that the catalyst is able to hold it's integrity for a long time pe-

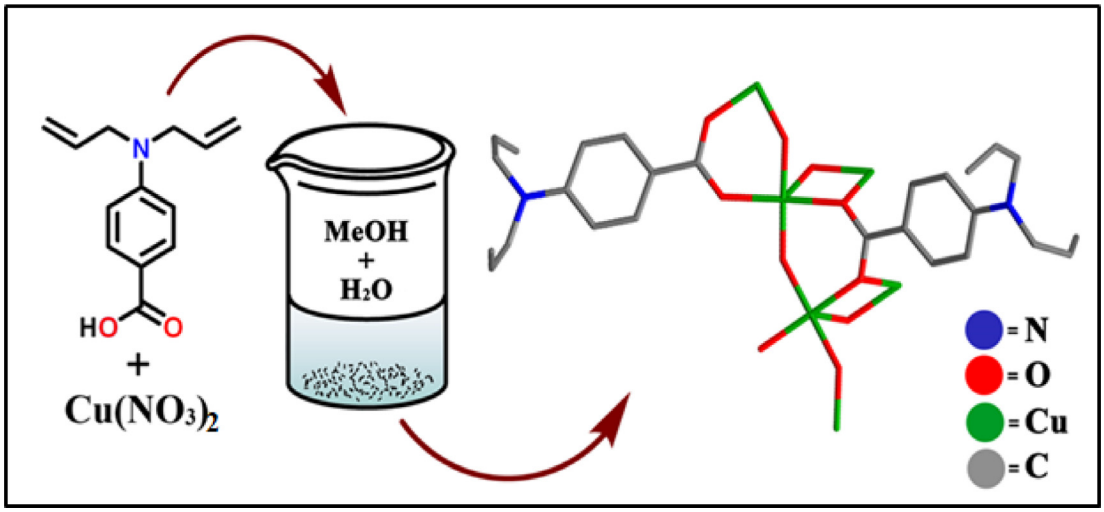

Scheme 1. Synthesis of the Coordination polymer $[Cu_2(\mu_2\text{–}OH)_2(DABA)_2]_n$ (1).

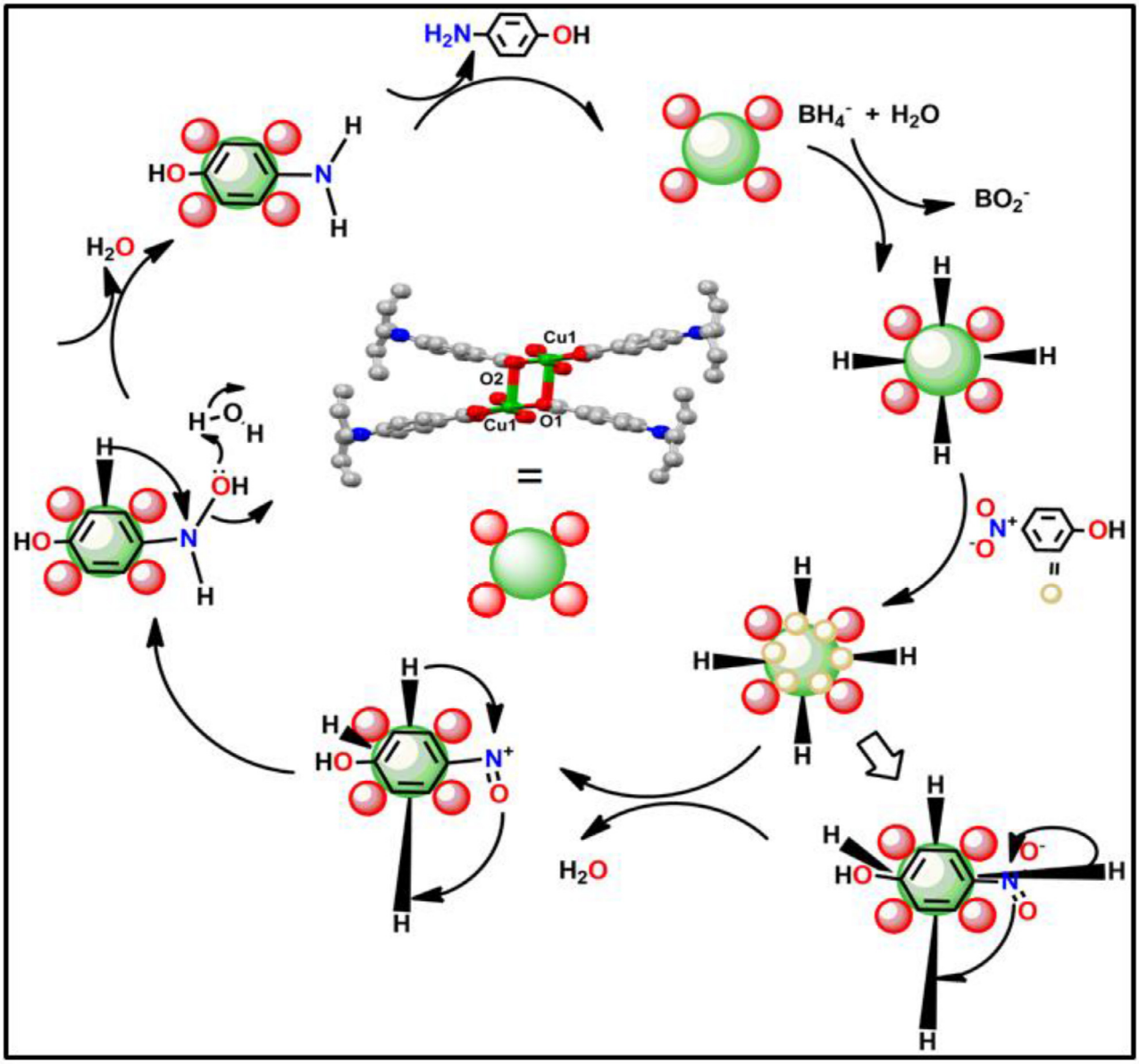

Scheme 2. Plausible mechanism for nitrophenol reduction by BH4– catalysed by nanopolymer.

riod (**Fig. S9**). Hence, we can say that the coordination polymer $[Cu_2(\mu_2\text{–}OH)_2(DABA)_2]_n$ (**1**), catalyst is successful in acting as an adsorbent catalyst in the reduction process.

4. Conclusion

In summary, a 1D coordination polymer of dinuclear Cu(II), $[Cu_2(\mu_2\text{–}OH)_2(DABA)_2]_n$ (**1**) (HDABA, 4-Diallylamino-benzoic acid) is structurally characterised who has useful catalytic efficiency for the reduction of nitrophenols to aminophenols by $NaBH_4$. Even after 6 cycling experiment, the catalytic activity for reduction was still noteworthy. Therefore, the recent discussions has further shown that we have successfully exhibited a facile green technique to synthesize nanoscale CP displaying as selective, sustainable as well as long term catalyst for nitroaromatic reduction. The magnetic study indicated the weak antiferromagnetic interaction in the reported compound.

Scheme 1 and 2.

Declaration of Competing Interest

The authors declare that they have no known competing financial interests or personal relationships that could have appeared to influence the work reported in this paper.

Acknowledgements

S. J would like to thank for the financial support to the Council of Scientific and Industrial Research (CSIR, Sanction no. 09/096(0858)/2016-EMR-I), New Delhi, India. M. S. E. F. acknowledges the financial support from the Spanish government (Grant PGC2018–094031-B-I00). S.K. is thankful to DST-INSPIRE [(No. DST/INSPIRE Fellowship/2018/IF180018 and Application Reference Number DST/INSPIRE/03/2017/001850)] for providing the fellowship. The authors wish to thank the University of Calcutta (CRNN) for providing the SEM facility.

Accession codes

CCDC 1896232 contain the supplementary crystallographic data for this paper. These data can be obtained free of charge via www.ccdc.cam.ac.uk/ data_request/cif, or by emailing data_request@ccdc.cam.ac. uk, or by contacting The Cambridge Crystallographic Data Centre, 12 Union Road, Cambridge CB2 1EZ, UK; fax: +441223 336033.

Supplementary materials

Supplementary material associated with this article can be found, in the online version, at doi:10.1016/j.molstruc.2021.131058.

References

[1] G. Wu, X. Liang, L. Zhang, Z. Tang, M. Al-Mamun, H. Zhao, X. Su, ACS Appl. Mat. Interf. 9 (2017) 18207.
[2] X. Qiao, Z. Zhang, F. Tian, D. Hou, Z. Tian, D. Li, Q. Zhang, Cryst.Grow. Desg. 17 (2017) 3538.
[3] M. Ismail, M. Khan, S. Khan, M. Khan, K. Akhtar, A. Asiri, J. Mol. Liq. 260 (2018) 78.
[4] A. Goyal, S. Bansal, S. Singhal, Int. J. Hydrogen Energy. 39 (2014) 4895.
[5] C. Lee, P. Alvarez, A. Nam, S. Park, T. Do, S.Lee U.Choi, J. Hazard. Mat. 325 (2017) 223.
[6] J. Wang, H. Lou, Z. Xu, C. Cui, Z. Li, K. Jiang, Y. Zhang, L. Qu, W. Shi, J. Hazard. Mat. 360 (2018) 356.
[7] L. Hao, T. Zheng, J. Jiang, G. Zhang, P. Wang, Chem. Eng. J. 292 (2016) 163.
[8] K. Shin, Y. Cho, J. Choi, K. Kim, Appl. Catal. A: General 413 (2012) 170.
[9] Y. Li, Y. Cao, J. Xie, D. Jia, H. Qin, Z. Liang, Catal. Commun. 58 (2015) 21.
[10] J.J. Lv, A.J. Wang, X. Ma, R.Y. Xiang, J.R. Chen, J.J. Feng, J. Mater. Chem. A. 3 (2015) 290.
[11] K. Sarmah, J. Pal, T.K. Maji, S. Pratihar, ACS Sustainable Chem. Eng. 5 (2017) 11504.
[12] X. Chen, Z. Cai, X. Chen, M. Oyamac, J. Mater. Chem. A. 2 (2014) 5668.
[13] X. Wang, D. Liu, S. Song, H. Zhang, J. Am. Chem. Soc. 135 (2013) 15864.
[14] Y. Fu, T. Huang, B. Jia, J. Zhu, X. Wang, Applied Catalysis B: Environmental 202 (2017) 430.
[15] T. Nguyen, C. Huang, R. Doong, Appl. Catal. B: Environ. 240 (2018) 337.
[16] Y. Fu, P. Xu, D. Huang, G. Zeng, C. Lai, L. Qin, B. Li, J. He, H. Yi, M. Cheng, C. Zhang, Appl. Surf. Sci. 473 (2019) 578.
[17] Y. Ma, X. Wu, G. Zhang, Appl. Catal. B: Environ. 205 (2017) 262.
[18] N. Sahiner, H. Ozay, O. Ozay, N. Aktas, Appl. Catal. B: Environ. 101 (2010) 137.
[19] B. Dutta, D. Das, J. Datta, A. Chandra, S. Jana, C. Sinha, P.P. Ray, M.H. Mir, Inorg. Chem. Front. 6 (2019) 1245.
[20] B. Dutta, A. Dey, C. Sinha, P.P. Ray, M.H. Mir, Inorg. Chem. 57 (2018) 8029.
[21] K. Naskar, S. Maity, S. Jana, B. Dutta, S. Tanaka, D. Mallick, T. Akitsu, C. Sinha, Cryst. Growth Des. 18 (2018) 2986.
[22] B. Dutta, R. Jana, C. Sinha, P.P. Ray, M.H. Mir, Inorg. Chem. Front. 5 (2018) 1998.
[23] H. Furukawa, K.E. Cordova, M. O'Keeffe, O.M. Yaghi, Science 341 (2013) 123.
[24] P. Silva, S.M.F. Vilela, J.P.C. Tome, F.A. Paz, Chem. Soc. Rev. 44 (2015) 6774.
[25] A.J. Howarth, Y. Liu, P. Li, Z. Li, T.C. Wang, J.T. Hupp, O.K. Farha, Nat. Rev. Mater. 1 (2016) 15018.
[26] A. Chandra, M. Das, K. Pal, S. Jana, B. Dutta, P.P. Ray, K. Jana, C. Sinha, ACS Omega. 4 (2019) 17649.
[27] N. Sakamoto, F.Y. Nishimura, T. Nonaka, M. Ohashi, N. Ishida, K. Kitazumi, Y. Kato, K. Sekizawa, T. Morikawa, T. Arai, ACS Catal. 10 (2020) 10412.
[28] D.P. Xu, M. Xiong, M. Kazemnejadi, RSC Adv. 11 (2021) 12484–12499.
[29] S. Jana, R. Jana, S. Sil, B. Dutta, H. Sato, P.P. Ray, A. Datta, T. Akitsu, C. Sinha, Cryst. Growth Des. 19 (2019) 6283.
[30] S. Jana, A. Ray, A. Chandra, E.S.M. Fallah, S. Das, C. Sinha, ACS Omega, 5 (2020) 274.
[31] BrukerSMART, SAINT. Software Reference Manual Bruker AXS Inc, Madison, Wisconsin, USA, 2000.
[32] G.M. Sheldrick, Acta Cryst A. A71 (2015) 3–8.
[33] L.J. Farrugia, *J. Appl.* Crystallogr 45 (2012) 849.
[34] K. Brandenburg, DIAMOND, Crystal Impact GbR, Bonn, Germany, 1999.
[35] S. Mukherjee, S. Ganguly, K. Manna, S. Mondal, S. Mahapatra, D. Das, Inorg. Chem. 57 (2018) 4050.
[36] S. Karim, S. Mukherjee, S. Mahapatra, R. Parveen, D. Das, **Biomater. Sci.** 9 (2021) 124–132.
[37] O. Kahn, Molecular Magnetism. VCH, 1993, p. 27.
[38] F. Novio, N.Vázquez-Mera J.Simmchen, D.Ruiz-Molina L.Amorín-Ferré, Coord. Chem. Rev. 25 (2013) 2839–2847.
[39] K. Roy, S. Jana, S.K. Ghosh, B. Mahanty, Z. Mallick, S. Sarkar, C. Sinha, D. Mandal, Langmuir 36 (2020) 11477–11489.
[40] B. Weber, Chem. Eur. J. 23 (2017) 18093 –18100.
[41] Z.D. Pozun, S.E. Rodenbusch, E. Keller, K. Tran, W. Tang, K.J. Stevenson, G. Henkelman, J. Phys. Chem. C. 117 (2013) 7598.
[42] M. Aghaei, A.H. Kianfar, M. Dinari, Appl. Organomet. Chem. 34 (2020) 5617.
[43] Y.A. Attia, Y.M.A. Mohamed, Appl. Organomet. Chem. 33 (2019) 4757.
[44] Z. Derikvand, F. Rahmati, A. Azadbakht, Appl. Organomet. Chem. 33 (2019) 4864.
[45] B.M. Hedayat, M. Noorisepehr, E. Dehghanifard, A. Esrafili, R. Norozi1, J. Mol. Liq. 264 (2018) 571.
[46] S. Ali, M.A. Farrukh, M. Khaleeq-ur-Rahman, Korean J. Chem. Eng. 30 (2013) 2100.